Finite size effects on Raman spectrum of single-walled boron nitride nanotube

B. Fakrach, A. Rahmani, H. Chadli and K. Sbai
Equipe de physique informatique et modélisation des systèmes, Université MY Ismail, Faculté des Sciences, BP 11201, Zitoune, 50000 Meknès, Morocco
J. L. Sauvajol
Laboratoire des Colloïdes, Verres et Nanomatériaux (UMR CNRS 5587), CP026, Université Montpellier II, 34095 Montpellier Cedex 5, France
Corresponding auther: email abdelali@fsmek.ac.ma

Using the spectral moments method, we present calculations of Raman active modes of Single Walled Boron Nitride Nanotube (SW-BNNT). The Spectra are computed for chiral and achiral nanotubes in terms of their diameter and length. The behaviors of low frequency Raman active modes characteristic, in terms of the tube diameter revealed that these frequencies are diameter dependent. We show that the number of Raman active modes, their frequencies, and intensities depend on the length and chirality of the nanotubes. These predictions are useful to interpret the experimental Raman spectra of BNNTs.

I. INTRODUCTION

Soon after the discovery of Single Walled Carbone Nanotube (SWCNT) [1] it was speculated that other materials could possibly form similar nanostrucures. Boron Nitride Nanotubes (BNNTs) were first predicted to be a stable structure based on tight-binding [2] and first-principal calculations [3]. The BNNT is diatomic species with its geometrical structure identical to that of SWCNT where boron and nitrogen atoms occupy the alternate nodes. The possibilities for technological applications of SW-BNNTs motivated the development of various methods for their production: arc discharge [4, 5], laser ablation [6, 7], and chemical vapor deposition [8]. A continuous laser vaporization process under a nitrogen atmosphere that produced BNNTs in gram quantities was reported [9]. The produced tubes have a finite length typically between 100-400 nm and appear either as individual tubes or as bundles where they are packed together through van der Waals inter-tubes interactions.

Vibrational spectroscopy especially Raman spectroscopy, has been shown to play a major role in carbon nanotube science [10]. At a theoretical level, the nonresonant Raman spectra of SWCNTs have been calculated within the bond polarizability model [11, 12]. It is expected that the combination of Raman and infrared spectroscopy will be a standard characterization tools for BNNTs. However, due to difficulties with the sample purification no experimental data on contamination-free samples have been reported. Electronic structure calculations indicated that the band gaps of BNNTs are insensitive to the diameter, chirality, and whether the tube is single walled, multi walled or packed into bundles [2, 3]. Measurements of the optical properties on a synthesized BN nanotube sample by means of absorption [13] and low-loss EELS [15] were performed and confirmed the predicted large band gap. Due to this latter large electronic band gap of the BNNTs, the Raman scattering of light is expected to be nonresonant in contrast to carbon nanotube in which the process is resonant. Raman experiments on unpurified BNNTs prepared by laser vaporization process have been reported [16]. Raman spectra were measured at different laser energies (457.9, 488, and 514.5 nm). Therefore, the resulting spectra are weaker in intensity and must be carefully separated from a possible overlap by resonant Raman scattering from contaminants. More recently, Raman spectroscopy of SW-BNNTs have been performed using visible and UV excitation energies. The authors show that in the visible range, the effect of contaminants is important, since it can hide the spectroscopic response of BNNTs. In the UV range, Raman scattering at 299 nm excitation wave length provides preresonant conditions and allows us to identify the tangential modes at high frequency (1370 cm^{-1}). In contrast to SWCNTs, no dependence on the excitation wavelength was observed confirming the insulating character of BNNTs.

Using a force constant model in which the interatomic force constants up to the fourth-nearest-neighbor interaction are fitted to experimental data, many calculations of phonons have been performed for graphite and carbon nanotubes [17, 18]. These approaches are very fast and allow a good understanding of phonon in nanotubes. The same approach was developed recently by Xiao *et al* for phonons in Boron nitride [19] and BC_3 [20] nanotubes. Group-theoretical analysis of single BNNTs [21] reveals that four A, five E_1 and six E_2 modes for chiral nanotubes, three A_g, five E_1, and six

E_2 modes for zigzag nanotubes, and three A_g, two E_{1g}, and four E_{2g} modes for armchair nanotubes are Raman active. The infrared and Raman active modes of individual single BNNTs have been predicted by different theoretical approches: zone-folding [22] combined with bond polarizability parameters of carbon [3, 4], tight binding approach [23], and *ab initio* calculations [24, 25]. From these studies, it is confirmed that the Radial breathing mode (RBM) in carbone nanotubes is inversely proportional to the tube diameter [18]. In BN nanotube, note only the RBM, but most of the low frequency modes display the same behaviour, i.e., $\omega_{RBM} = A/D$, the constant A is a model dependent, A ≈ 2182 cm^{-1}Å from tight-binding model [23], A ≈ 1902 cm^{-1}Å from force constant model [19] and A ≈1702 cm^{-1}Å from valance shell model [22] and A ≈ 515 cm^{-1}Å from density functional theory [26].

In this work, we present calculation results of the nonresonant Raman spectra in the breathing like modes (BLM) range and tangential-like modes (TLM) one of single wall boron nitride nanotube. These calculations have been performed for a large collection of infinite nanotubes with various diameter and chirality. Thanks to the spectral moments method, we have investigated the finite length effects on SW-BNNT Raman spectra.

II. MODELS AND METHODS

A SW-BNNT structure can be considered in quite the same way as it was done for SWCNT [17] by rolling a single hexagonal BN sheet. Such a tube can uniquely be specified by the pair of integers (n,m) that define the lattice translation vector. The interatomic interactions at the surface of the SW-BNNT are described by using the force constants model introduced by Xiao [19].

The spectral moments method (SMM) was shown to be a powerful tool for determining infrared absorption, Raman scattering, and inelastic neutron-scattering spectra of harmonic systems [28]. In our previous work on the nonresonant Raman spectrum on finite and infinite SWCNTs, we have successfully calculated the Raman spectra for achiral and chiral SWCNTs in a large range of diameters and lengths (up to 80 nm) [12]. This same approach has been recently used to calculate the dependence of the Raman spectrum of double-walled carbon nanotubes as a function of the diameter and chirality of the inner and outer tubes [12].

The Raman scattering of light is expected to be nonresonant for BN nanotubes. Therefore, the Raman scattering cross section can be calculated assuming the induced polarization tensor is known [29]. In this paper, the Raman cross section was calculated assuming that scattering can be described within the framework of the bond polarizability model. In that case, the polarization is only modulated by the nearest-neighbor bonds and the components of the induced polarizability tensor are given by the empiric equation [30,31]

$$\pi_{\alpha\beta}(r) = \frac{1}{3}(\alpha_l + 2\alpha_p)\delta_{\alpha\beta} + (\alpha_l - \alpha_p)(\hat{r}_\alpha \hat{r}_\beta - \frac{1}{3}\delta_{\alpha\beta})$$

Where α and β are related to the Cartesian components (x, y, z) and $\hat{r}$ is the unit vector along the vector $\vec{r}$ connecting atom n and atom m which are covalently bonded. The parameters α_l and α_p correspond to the longitudinal and perpendicular bond polarizability respectively. Within this approach, one can assume that the bond polarizability parameters are related to the bond lengths r only. The derivatives $\pi^n_{\alpha\beta,\gamma}$ are given by:

$$\pi^n_{\alpha\beta,\gamma} = \sum_m \frac{1}{3}(\alpha'_p + 2\alpha'_l)\delta_{\alpha\beta}\hat{r}_\gamma + (\alpha'_l - \alpha'_p)(\hat{r}_\alpha \hat{r}_\beta - \frac{1}{3}\delta_{\alpha\beta})\hat{r}_\gamma + \frac{\alpha_l + 2\alpha_p}{r}\left(\delta_{\alpha\gamma}\hat{r}_\beta + \delta_{\beta\gamma}\hat{r}_\alpha - 2\hat{r}_\alpha \hat{r}_\beta \hat{r}_\gamma\right)$$

Where $\alpha' = \left(\frac{\partial \alpha}{\partial r}\right)_{r=ro}$ and r_0 is the equilibrium bond distance. The Raman intensities are calculated using the bond polarizability parameters of carbon [27].

III. RESULTS AND DISCUSSION

In this section we report calculations result for the polarized nonresonant Raman spectra of achiral and chiral of single-wall Boron nitride nanotubes of different diameters and chiralities using the spectral moments method. The mode frequency is directly obtained from the position of the peak in the calculated Raman spectrum. In all our calculations, we consider that the Z nanotube axis is to be along z axis, and the X nanotube axis is to be along the x axis of the laboratory reference frame. The laser beam is kept along the y axis. Three geometrical configurations are considered: in the ZZ configuration, both incident and scattered polarizations are along the Z axis and, for ZX (XY)

configuration, the incident and scattered polarizations are along the Z(X) and X(Y) axes respectively.

A. Polarized Raman spectra of infinite crystals of SW-BNNTs

In this section, calculations of the Raman spectra for achiral (armchair and zigzag) and chiral nanotubes are performed for infinite crystal of nanotubes by applying periodic conditions of nanotubes unit cell. In Figure1, we show the polarized calculated ZZ, ZX and XY Raman spectra of infinite (10,10)(bottom), (17,0)(midle), and (14,7)(top) nanotubes, whose diameters are 1.37 nm, 1.35 nm and 1.47 nm, respectively. The spectra are displayed in the BLM and TLM regions.

In the BLM region (lower than 500 cm^{-1}), first for (10,10) armchair tube a single A_1 mode is observed in the ZZ polarization, a single E_1 is active in the ZX and two E_2 in the YX. The number and the symmetry of these modes is the same as infinite SWCNT independently to its chirality [12]. For (17,0) zigzag and (14,7) chiral tubes, a single A_1 mode is active in the ZZ polarization , two E_1 are active in ZX, and three E_1 are observed in YX. The chiral and zigzag BN tubes show one E_1 and E_2 additional Raman active modes in comparaison with SWCNTs [12].

In the (600-1200 cm^{-1}) intermediate-frequency region, three weak modes: A_{1g} at 718 cm^{-1}, E_{1g} at 714 cm^{-1} and E_{2g} at 703 cm^{-1} (A_1, 711 cm^{-1}, E_1, 709 cm^{-1} and E_2, 700 cm^{-1}), are observed respectively in ZZ, ZX and YX spectra of (17,0) ((14,7)) nanotube. For (10,10) nanotube, only two weak A_{1g} and E_{2g} modes located at 707 cm^{-1} and 695 cm^{-1} respectively are Raman active.

Concerning TLM region, the polarized calculated spectra show two peaks for chiral and one peak for achiral SW-BNNTs. In the case of zigzag tube, spectra show one peak with a small intensity for ZX and XY polarizations. The calculated frequencies of A_{1g}, E_{1g} and E_{2g} tangential modes can be pointed out: A_{1g} at 1359 cm^{-1}, E_{1g} at 1417 cm^{-1} and E_{2g} at 1370 cm^{-1} for (10,10) SW-BNNT; A_{1g} at 1427 cm^{-1}, E_{1g} at 1368 cm^{-1}, 1423 $cm^{-1}$and E_{2g} at 1375 cm^{-1}, 1413 cm^{-1} for (17,0) SW-BNNT; and A at 1360 cm^{-1}, 1425 cm^{-1}, E_1 at 1363 cm^{-1}, 1423 cm^{-1} and E_2 at 1370 cm^{-1} for (14,7) SW-BNNT.

B. Chirality dependence of the Raman spectrum of infinite SW-BNNT

To investigate the chirality dependence of the Raman active modes of SW-BNNT, we have considered different values of the chiral angle θ. In Figure.2, we show the TLM region of the ZZ (top), ZX (middle) and YX (bottom) Raman spectra of infinite SW BNNTs for five values of θ (0°, 10°, 15°, 20° and 30°), associated with (17,0), (17,3), (14,5), (14,7) and (10,10) nanotubes, whose diameters are 1.35 nm, 1.48 nm, 1.35 nm, 1.47 nm and 1.37 nm, respectively. The calculation results mainly illustrate the chirality dependence of the TLM Raman spectra profile. For these nanotubes with similar diameters, no difference is observed in the BLM frequency region in comparing with TLM ones which is very sensitive to the tube chirality. For the armchair tube (θ = 30°), each polarized spectrum is featured by a single peak assigned to A_{1g}(ZZ), E_{1g}(ZX) and E_{2g}(YX) tangential modes, respectively, as compared to two peaks for each polarized spectrum in chiral (0° < θ < 30°) BNNTs. For zigzag tube (θ = 0°), spectra show two peaks for ZX (E_{1g}), XY (E_{2g}) symmetry and one peak for ZZ (A_{1g}) symmetry.

C. Diameter dependance of the frequency of the radial breathing modes region

We have investigated the dependence of the Raman spectrum of SW-BNNT in relation to diameter. We have calculated polarized Raman spectra in a large diameter range. From this work, it is shown that the low frequency modes are likely the most influenced modes by the diameter variation in comparison to the intermediate and high frequency ones. The radial breathing mode (RBM) for (10,10) SW-BNNT frequency is located at 138 cm^{-1}. In Figure3, we plot the diameter dependence of the frequency of the radial breathing modes region (A_{1g}, E_{1g}, E_{2g}), for tubes (chiral and achiral) with diameter between 6 and 15 Å. The dependence of the RBM frequency on the diameter was fitted with a simple power law: $\omega_{RBM} = A/D$, where A ≈ 1899 cm^{-1}Å. This value of fitting constant A is consistent with that in Refs. [23,32] and approximately equal that in Ref. [19] (A ≈ 1902 cm^{-1}Å).

D. Polarized Raman spectra of finite length SW-BNNTs

The finite nature of the tube length was found to be an important feature for using nanotubes in industrial applications [33]. It is thus of great interest to investigate the vibrational properties of nanotubes with a finite length. A few years ago, a theoretical study of finite-size effects on the Raman spectrum of SWCNT was performed [12, 34]. In the present work, we calculate the Raman intensity of the finite length nanotube with open ends without any terminations. The analysis of SW-BNNT for larger length range (from 10 to 900 Å), closer to reality, as well as for achiral and chiral tubes of different diameters is performed.

To illustrate the dependence of the Raman-active modes on the tube length, in Figure 4, the dependences of polarized Raman spectra in the BLM and TLM frequency range are displayed as a function of the nanotube length L for (10,10), (17,0), and

(14,7) SW-BNNTs. For all chiralities, we found an increase in the number of Raman active modes when the tube length decreases. Moreover, the relative intensities of peaks are significantly length dependent. The frequencies of the principal modes are the same ones as those calculated for the tubes of infinite length. The additional modes are observed at low frequency for short tubes, and their frequencies are significantly depending on the tube length. All these modes were missing for very long and infinite nanotubes. We observe that the most significant effect of finite size occurs in the intermediate range, 500-1100 cm^{-1}, where a large number of peaks are predicted to be Raman active, especially for $A(A_{1g})$ symmetry, and mainly for tube lengths below 200 Å. Most of these peaks vanish for lengths greater than 500 Å.

IV. CONCLUSION

In this work we have presented calculation results for the polarized nonresonant Raman spectra of single-walled BN nanotubes of different diameters and chiralities using the spectral moments method in the framework of polarisation theory. The frequencies of Raman active modes in zigzag, chiral, and armchair tubes in terms of tube diameter and chirality are presented. Our results show that the radial breathing mode frequency is inversely proportional to the nanotube diameters and there is no chirality effect on Raman spectra for BNNT diameters lower than 15 Å, which is in good agreement with previous theoretical results. Concerning the finite size effects, we show that the number of Raman-active modes increases as soon as the tube length decreases particularly in the intermediate region. These additional peaks are missing for very long and infinite nanotubes. These predictions must be very useful to interpret experimental spectra for BN nanotubes.

V. ACKNOWLEDGEMENTS

The works was supported by a CNRS-France/CNRST-Morocco agreement.

REFERENCE:

[1] S.Iijima, Nature (London)56, 354 (1991).
[2] A. Rubio, J. L. Corkill, and M. L. Cohen, Phys. Rev. B 49, 5081 (1994).
[3] X. Blase, A. Rubio, S. G. Louie, and M. L. Cohen, Europhys. Lett. 28, 335 (1994).
[4] N. G. Chopra, J. Luyken, K. Cherrey, V. H. Crespi, M. L. Cohen, S. G. Louie, and A. Zettl, Science 69, 966 (1995).
[5] Y. Saito, M. Maida, and T. Mastumoto, Jpn. J. Appl. Phys. 38, 159 (1999).
[6] D. Golberg, Y. Bando, M. Eremets, K. Takemura, K. Kurashima, and H. Yusa, Appl. Phys. Lett. 69, 2045 (1996).
[7] D. P. Yu, X. S. Sun, C. S. Lee, I. Bello, S. T. Lee, H. D. Gu, K. M. Leung, G. W. Zhou, Z. F. Dong, and Z. Zhang, Appl. Phys. Lett. 72, 1966 (1998).
[8] O. R. Lourie, C. R. Jones, B. M. Bartlett, P. C. Gibbons, R. S. Ruoff, and W. E. Buhro, Chem. Mater. 12, 1808 (2000).
[9] R. S. Lee, J. Gavillet, M. Lamy de la Chapelle, A. Loiseau, J.-L.Cochon, D. Pigache, J. Thibault, and F. Willaime, Phys. Rev. B 64,121405(R) (2001).
[10] M.S.Dressellhaus and P. C. Eklund, adv. Phys. 49,705 (2000).
[11] R. Saito, T. Takeya, T. Kimura, G.Dresselhaus, and M.S.Dressellhaus, Phys. Rev. B 57, 2555 (1999).
[12] A. Rahmani, J.L. Sauvajol, S. Rols and C. Benoit, Phys. Rev. B 66, 125404 (2002).
[13] J. S. Lauret, R. Arenal, F. Ducastelle, A. Loiseau, M. Cau, B.Attal- Tretout, E. Rosencher, L. Goux-Capes, Phys. Rev. Lett. 94 037405 (2005)
[15] R. Arenal, O. Stephan, M. Kociak, D. Taverna, A. Loiseau, C. Colliex, Phys. Rev. Lett. 95, 127601. (2005)
[16] R. A. de la Concha, L. Wirtz, J.Y. Mevellec, S. Lefrant, A. Rubio, A. Loiseau, Electronic Properties of Novel Materials: XVIIth International Winterschool, Ed. H. Kuzmany, J. Fink, M. Mehring and S. Roth, World Scientific, Singapure , (2003)
[17] R. Saito, G. Dresselhaus, and M.S. Dresselhaus , Physical properties of carbon nanotubes (Imperial college Press, London,1998)
[18] R.A. Jishi, L. Venkataraman, M.S. Dresselhaus, and G. Dresselhaus,Chem. Phys. Lett. 209, 77 (1993).
[19] Y. Xiao, X. H. Yan, J. X. Cao, J. W. Ding, Y. L. L. Mao, and J. Xiang, Phys. Rev. B 69, 205415 (2004)
[20] Z. X. Guo, Y. Xiao, J. W. Ding, and X. H. Yan, Phys. Rev. B 73, 045405 (2006).
[21] O. E. Alon, Phys. Rev. B 64, 153408 (2001).
[22] V.N.Popov, Phys. Rev. B 67, 085408 (2003).
[23] D. Sanchez-Portal and E. Hernandez, Phys. Rev. B 66, 235415 (2002).
[24] L. Wirtz, M. Lazzeri, F.Mauri, and A.Rubio, Phys. Rev. B 71, 241402(R)(2005).
[25] L. Wirtz and A. Rubio, Phys. Rev. B 2, 4 (2003).
[26] L. Wirtz, A. Rubio, R.A. de la Concha, and A. Loiseau, Phys. Rev. B 68, 045425 (2003).
[27] R. Saito, T. Takeya, T. Kimura, G. Dresselhaus, and M. S. Dresselhaus Phys. Rev. B 57, 4145 (1998).
[28] C. Benoit, E. Royer, and G. Poussigue, J. Phys.: Condens. Matter 4, 3125 (1992).

[29] Light Scattering in Solids II, edited by M. Cardona and Gntherodth Springer-Verlag, Berlin, (1982).
[30] R. J. Bell, Methods in Computational Physics, Vol. 15, Academic,New York, (1976).
[31] S. Guha, J. Menendez, J. B. Page, and G. B. Adams, Phys. Rev. B 53, 13106 (1996).
[32] B. Akdim, Sankar P.Sanyal, Physica E 24, 244 (2004).
[33] S.J. Tans, Verchueren, and C.Dekker,Nature (London) 49 393 (1998).
[34] R. Saito, T. Takeya, T. Kimura, G. Dresselhaus and M.S. Dresselhaus Phys. Rev. B 59, 2388 (1999).

FIGURE CAPTIONS

FIG. 1: The Polarized Raman spectra of (10,10) (bottom), (17;0) (middle), and (14,7) (top) BNNT crystals.

FIG. 2: The dependence of polarized Raman spectra of BNNT crystals in the TLM range as a function of the chiral angle θ.

FIG. 3: the diameter dependence of the frequency of the radial breathing modes region (A_{1g} , E_{1g} , E_{2g}), for tubes (chiral and achiral) with diameter between 6 and 15 Å.

FIG. 4: Dependence of the polarized Raman spectrum as a function of the tube length: top, (10,10), middle (17,0), and bottom (14,7) SW-BNNTs.

TABLES

Table 1: Force-constant parameters for 2D h-BN in units of 10^4 dyn/cm.

Radial	Tangential	
$\phi_r^{(1)} = 31.00$	$\phi_{ti}^{(1)} = 18.50$	$\phi_{to}^{(1)} = 5.60$
$\phi_r^{(B-B)} = 7.00$	$\phi_{ti}^{(B-B)} = -3.23$	$\phi_{to}^{(B-B)} = -0.70$
$\phi_r^{(N-N)} = 8.00$	$\phi_{ti}^{(N-N)} = -0.73$	$\phi_{to}^{(N-N)} = -0.55$
$\phi_r^{(3)} = 1.00$	$\phi_{ti}^{(3)} = -3.25$	$\phi_{to}^{(3)} = 0.65$
$\phi_r^{(4)} = -1.90$	$\phi_{ti}^{(4)} = 1.29$	$\phi_{to}^{(4)} = -0.30$

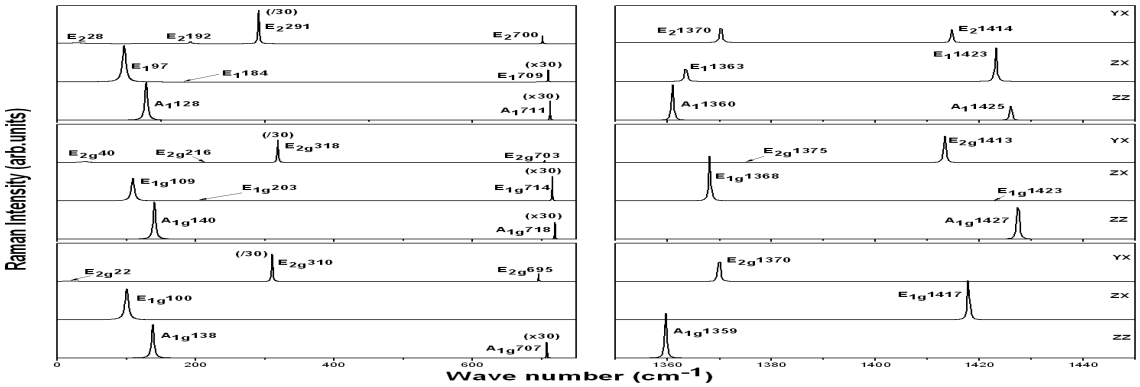
Raman Intensity (arb.units)
Wave number (cm-1)
ZZ
ZX
YX

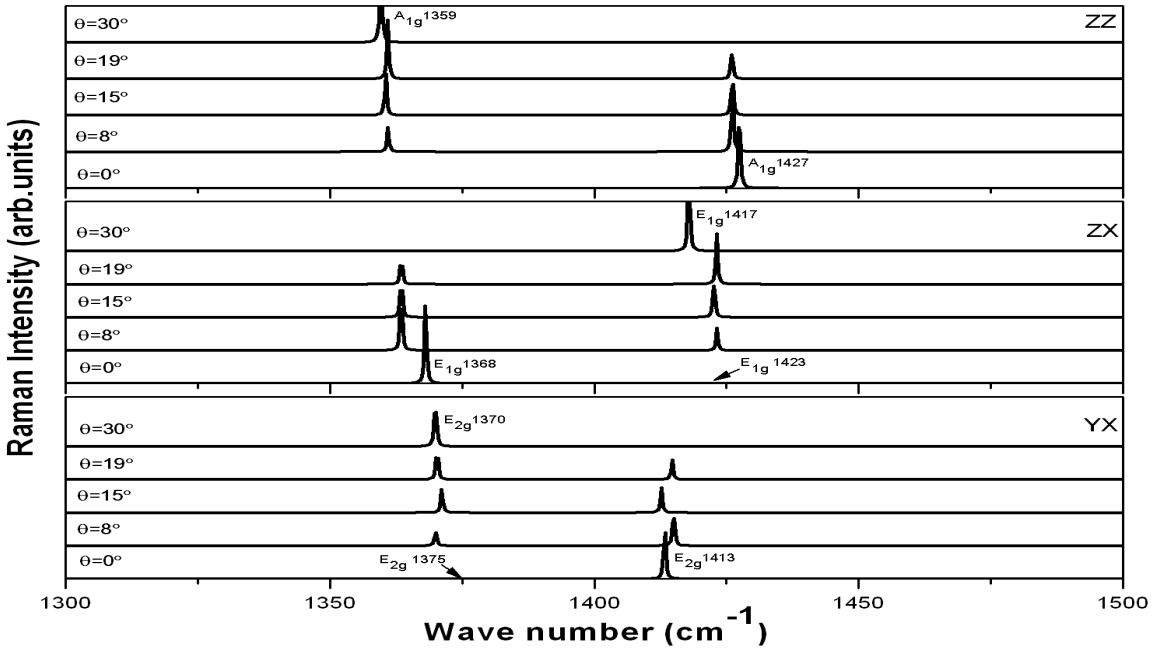
Raman Intensity (arb.units)
θ=30°
θ=19°
θ=15°
θ=8°
θ=0°
ZZ
ZX
YX
Wave number (cm-1)

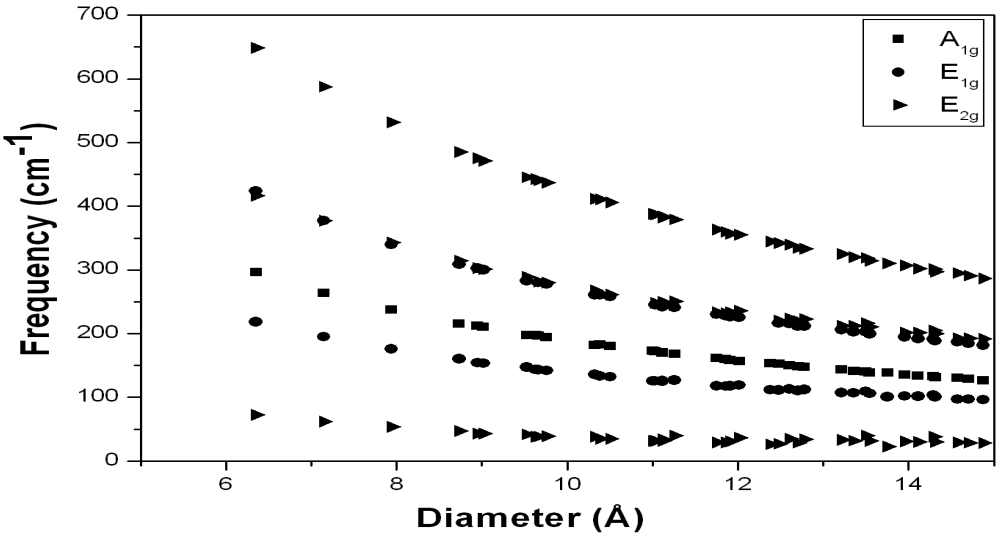
Frequency (cm-1)
Diameter (Å)

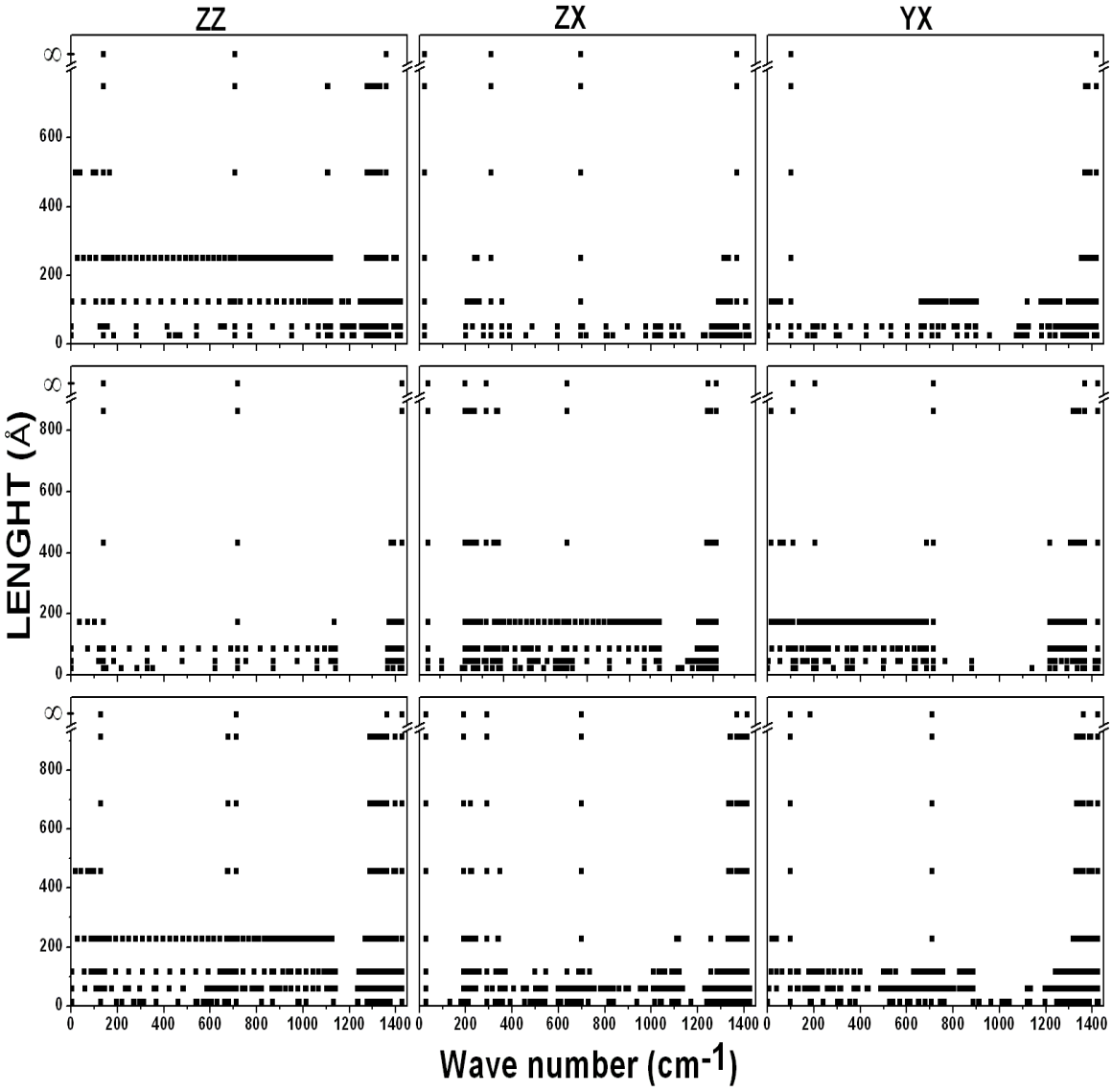
ZZ
ZX
YX
LENGHT (Å)
Wave number (cm-1)
0
200
400
600
800
1000
1200
1400
∞